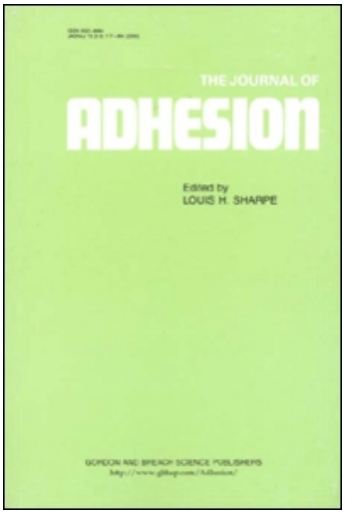

The Journal of Adhesion
Publication details, including instructions for authors and subscription information:
http://www.informaworld.com/smpp/title~content=t713453635

Effect of Moisture on the Contact between a Cylinder and a Parallel Plate

James C. M. Li[a]; Chenny Zhenyu Wang[a]
[a] Department of Mechanical Engineering, University of Rochester, Rochester, New York, USA

To cite this Article Li, James C. M. and Wang, Chenny Zhenyu(2005) 'Effect of Moisture on the Contact between a Cylinder and a Parallel Plate', The Journal of Adhesion, 81: 10, 1049 — 1073
To link to this Article: DOI: 10.1080/00218460500310788
URL: http://dx.doi.org/10.1080/00218460500310788

The Journal of Adhesion, 81:1049–1073, 2005

ISSN: 0021-8464 print/1545-5823 online
DOI: 10.1080/00218460500310788

Taylor & Francis
Taylor & Francis Group

Effect of Moisture on the Contact between a Cylinder and a Parallel Plate

James C. M. Li
Chenny Zhenyu Wang
Department of Mechanical Engineering, University of Rochester, Rochester, New York, USA

The problem of adhesion between a cylinder and a plate with a water bridge in between is solved exactly. The adhesive force needed to separate the cylinder and plate at constant volume of water or at constant humidity is shown to be different and both are unstable except for a small distance at constant volume. For large contact angles and constant volume of water the curvature of the water/air interface can change sign during separation. Increasing the contact angles between water and cylinder or between water and plate reduces the adhesive force. The adhesive force decreases with increasing humidity. The experiment, which used silicone oil instead of water, to keep volume constant, agrees with the calculations.

Keywords: Adhesion; Moisture; Cylinder/Plate; Water-bridge; Contact angle; Silicone oil

INTRODUCTION

Most solid surfaces exposed to air are covered with water molecules because air is usually moist. Hence, when two solid surfaces contact each other, their interaction must involve this layer of water molecules. In fact, direct solid/solid contact is nonexistent in moist air. The relative humidity needed for the water layer to exist could be very small. It is less than 1% if the separation between the two solid surfaces is in the atomic dimensions. Reports on the effect of relative

Received 8 November 2004; in final form 13 June 2005.
One of a collection of papers honoring Manoj K. Chaudhury, the February 2005 recipient of The Adhesion Society Award for Excellence in Adhesion Science, sponsored by 3M.
Address correspondence to James C. M. Li, Department of Mechanical Engineering, University of Rochester, Rochester, NY 14629, USA. E-mail: li@rochester.edu

humidity on the adhesion between solid surfaces are varied [1–20]. Some found the adhesion force increases with relative humidity [1–3, 5–11, 13–15, 17–19], some found it decreases with increasing relative humidity [7, 9–11, 13, 14, 17], and some found no effect [1, 2, 4, 7–13, 15–17, 20]. For example, Sedin and Rowlen [11] reported the pull-off force between an Si_3N_4 tip and a mica surface increased with increasing relative humidity (RH) between 0 and 60%. Although their results are similar to those of Thundat *et al*. [19] for the same system, both were drastically different from those of Hu *et al*. [17]. The latter group found for the same system very little pull-off force below 20% RH. Starting at about 20% RH the pull-off force increased sharply to a maximum of 7 nN at 30% RH and then decreased continuously all the way to about 2.5 nN at 90% RH. On the other hand, Eastman and Zhu [16] found that the pull-off force between a mica surface and either a bare Si_3N_4 tip, a gold-coated tip (higher pull-off force), or a paraffin-coated tip (lower pull-off force) did not change much with RH between 25 and 85%. Very little was offered to explain these differences. As observed by Opalinski [21], there is no agreement between model predictions and experimental results both for values and trends of adhesion forces.

As another example, He *et al*. [9] found that the pull-off force between a 3.7-μm glass sphere and a flat Si surface increases with RH between 10 and 50%. For the pull-off force between a hydrophilic tip and a flat CaF_2 surface, it increased from 10–20% relative humidity and then decreased all the way to 80% relative humidity. However, the pull-off force between a sharp SFM (scanning force microscopy) tip coated with OTS (n-octadecyl-trichloro-silane) and a flat Si surface did not change with RH between 10 and 80%. Similar results were reported earlier by Eastman and Zhu [16], who found within experimental error no effect of moisture between 25 and 85% RH for a bare Si_3N_4 tip or gold- and paraffin-coated tips contacting a mica surface. No explanation was offered in all these cases.

One of the reasons for the lack of agreement between theory and experiment is the difficulty in calculating the adhesive forces. For example, Marmur [22] assumed a circular arc of the water bridge in the cross section including the axisymmetric axis between a sphere and a plate. He also neglected the capillary force exerted by the water/air interface, as pointed out by de Lazzer *et al*. [23]. The trouble with the circular arc approximation [9, 11, 21–24] is that there is no way to estimate the errors caused by it.

In this article we examine the case of the cylinder/plate contact with a water bridge, a two-dimensional problem, so that exact calculations are possible. Admittedly, it is different from the sphere/plate

contact problem. In fact Chaudhury *et al*. [25] already have shown the difference between the sphere/plate contact and the cylinder/plate contact even without moisture. For example, the pull-off force is independent of the moduli of the materials in the case of sphere/plate contact but it is dependent for the cylinder/plate contact. However, such difference does not apply to contact adhesion with a water bridge. Furthermore, we learn a lot from this simpler case of the cylinder/plate contact so as to sort out the answers for this complex nonlinear problem before we approach the sphere/plate contact problem. All the features are examined in detail. The results will be useful in repeating and comparing these features with the case of the sphere/plate contact, which will be reported in a subsequent publication. A series of experiments are performed to test the adhesion-force behavior with respect to separation at a constant volume of silicone oil.

THE PROBLEM AND THE VARIABLES

As seen in Figure 1, a water bridge is formed between a cylinder of radius R and a plane surface. The contact angle between water and the cylinder surface is θ_1 and that between water and the plane surface is θ_0. This is a two-dimensional problem, so the water/air interface is cylindrical with a radius r, which is determined by the RH as follows:

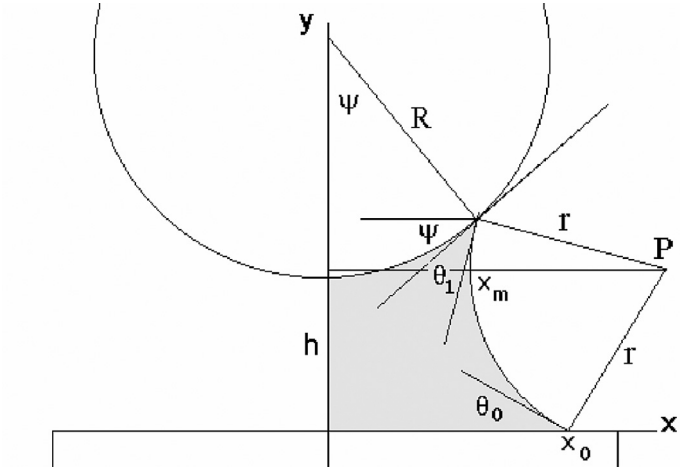

FIGURE 1 Cylinder/plate adhesion with water bridge.

$$r = -\frac{\gamma_{WA}\Omega}{\Re T \ln(p/p_0)} \tag{1}$$

where γ_{WA} ($0.073\,\mathrm{J/m^2}$ at room temperature) is the free energy of the water/air interface, which, when divided by r, is equivalent to a pressure applied over the water surface. The pressure here is negative because the surface is concave for water. A negative sign is introduced to make r positive. Ω is the molar volume of water, 18 cc/g-mol at room temperature, T is the absolute temperature, and p is the partial pressure of water, whereas p_0 is the partial pressure at saturation (at T) so p/p_0 is the relative humidity at T. $\Re$ is the gas constant, 8.314 J/g-mol. It is seen that at room temperature, although r is zero at zero humidity and infinity at 100% RH, it is only about 1 nm at 50% relative humidity. The calculated results are shown in Table 1 at room temperature (298 K). With all these variables given, the problem is to find the force–separation relation.

Several geometrical relations can help us compute the radius of curvature of the water/air interface. For example, from the (x,y) coordinates of the center point, P,

$$R\sin\psi + r\sin(\psi + \theta_1) = x_0 + r\sin\theta_0 \tag{2}$$

$$h + R - R\cos\psi - r\cos(\psi + \theta_1) = r\cos\theta_0. \tag{3}$$

The volume of water per unit length of cylinder is twice the shaded area shown in Figure 1 and is given by

TABLE 1 Relation between Relative Humidity and Radius of Curvature

r, nm	RH (%)
0.1	0.5
0.12	1
0.18	5
0.23	10
0.38	25
0.76	50
1.84	75
5.0	90
10.3	95
52.7	99
105.8	99.5

$$V = (R\sin\psi + x_0)(h + R - R\cos\psi) - R^2\psi + R^2\sin\psi\cos\psi + r^2\sin(\psi + \theta_0 + \theta_1) - r^2(\pi - \psi - \theta_0 - \theta_1). \quad (4)$$

The known quantities are R, h, V, θ_0, and θ_1 so there are only three unknowns, ψ, r, and x_0, which can be solved from the three equations. If the RH or r is known, V becomes unknown, so there are still three unknowns. To solve these equations care should be taken to avoid the two sides of the water/air interface becoming overlapped at increasing separation. These equations do not prevent such overlap and will give erroneous answers when that happens. To avoid such an overlap, the smallest coordinate of the water/air interface is calculated:

$$x_m = R\sin\psi + r\sin(\psi + \theta_1) - r \quad (5)$$

and it should always be positive.

The adhesive force per unit length in the z direction required to maintain the separation at h between the cylinder and the plate is given by

$$\frac{F}{\gamma_{WA}} = \frac{2R\sin\psi}{r} + 2\sin(\psi + \theta_1). \quad (6)$$

This force has two parts expressed as the two terms on the right side of Equation (6). The first one is to overcome the negative pressure created by the curvature of the water/air interface and the second one is due to the surface tension at the cylinder/water/air intersection. This consideration is from the cylinder side. From the plate side, it should be

$$\frac{F}{\gamma_{WA}} = \frac{2x_0}{r} + 2\sin\theta_0. \quad (7)$$

Equations (6) and (7) are, of course, the same because of Equation (2).

SEPARATION AT CONSTANT VOLUME OR AT CONSTANT HUMIDITY

To see how the adhesive forces change with the separation, h, it is necessary to know whether the volume of water or the curvature of the air/water interface is kept constant. If the volume of water is kept constant by, for example, a separation process fast enough to prevent water from evaporating into, or condensing from, the vapor and yet slow enough to allow the water bridge to change shape, there will be no equilibrium between the water vapor and the water bridge. However,

the air/water interface still will be cylindrical because of the minimization of surface energy (to be proved in a later publication). Now, if the curvature of the air/water interface is kept constant by, for example, a separation process slow enough to allow equilibrium between the water vapor and the air/water interface and the RH is kept constant all the time, the volume of water will change because of evaporation or condensation. In an actual experiment, both are possible. It may depend on how fast the cylinder is pulled away from the plate.

Figure 2 shows the situation at constant volume of water ($0.3\,R^2$ per unit length of cylinder) for zero contact angles at both the water/cylinder/air contact and the water/plate/air contact. Note that the radius of curvature, which started at $0.377R$, decreases to a minimum of $0.236R$ at $h = 0.25R$ and then increases again. Note also that x_m, the shortest distance of the water/air interface from the center plane, started at $0.851R$ and decreases continuously until it hits zero at $h = 1.246\ R$ at which time the bridge is broken. Yet there is no sign of this event from the other curves.

Figure 3 shows the situation at constant curvature of the water/air interface (radius is $0.377R$) maintained by constant humidity. The

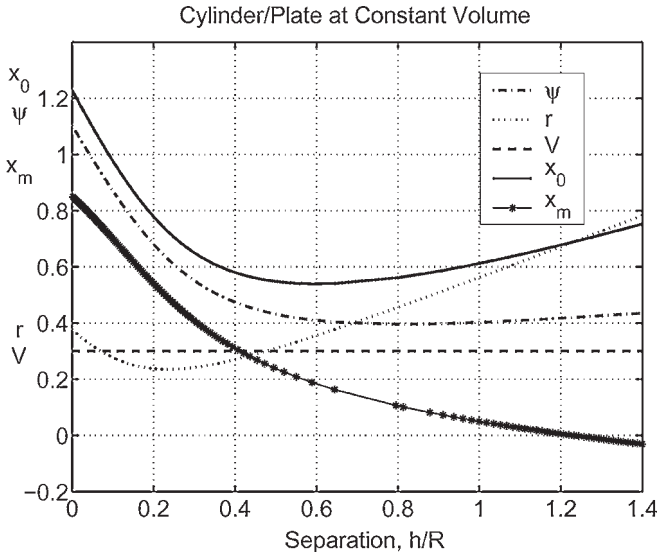

FIGURE 2 Configuration changes of water bridge when the cylinder is pulled away from the plate while maintaining the volume of water constant at $0.3R^2$ per unit length of cylinder.

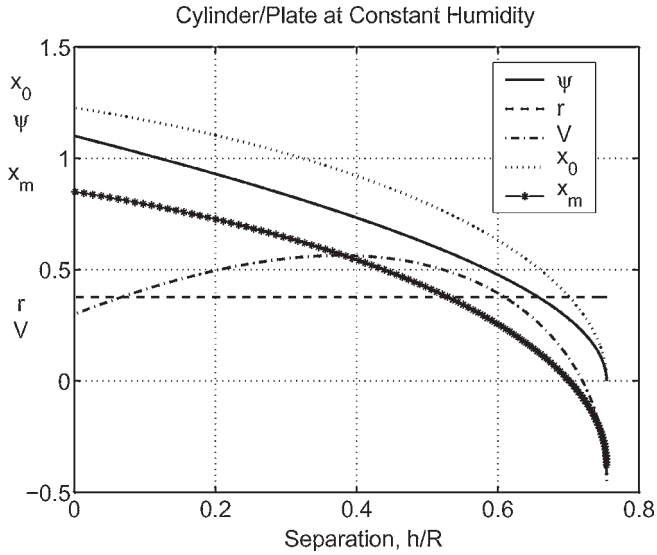

FIGURE 3 Configuration changes of water bridge when the cylinder is pulled away from the plate while maintaining the curvature of the water/air interface because of constant humidity.

contact angles are again assumed zero. Note that the volume of water that started at $0.3\,R^2$ per unit length of cylinder increased to $0.564\,R^2$ at $h = 0.4R$ and decreases again. Note also that x_m, the shortest distance of the water/air interface from the center plane, started at $0.851R$ and decreases continuously until it hits zero at $h = 0.7\,R$ at which time the water bridge is broken. Yet there is no warning of this event from the behavior of the other curves.

The difference between the two situations shows up also in the adhesive forces which are shown in Figure 4. The force is in units of γ_{WA}, the interfacial energy between water and air. It is seen that at constant volume of water, the forces increases first with separation, reaching a maximum, and then decreases. When it reaches 2 at $h = 1.25R$, the water bridge is broken; and suddenly the force would become zero. There is no sign of this event in this plot. For constant radius of curvature, which is maintained at $0.377R$ by the RH, the adhesive force decreases with separation from the beginning and reaches 2 at $h = 0.7R$ when the water bridge is broken and the force becomes zero suddenly. Here again there is no sign of such an event from this plot. These results show that when a numerical calculation is made for the case of sphere/plate contact, care must be exercised for the breakage of the water bridge.

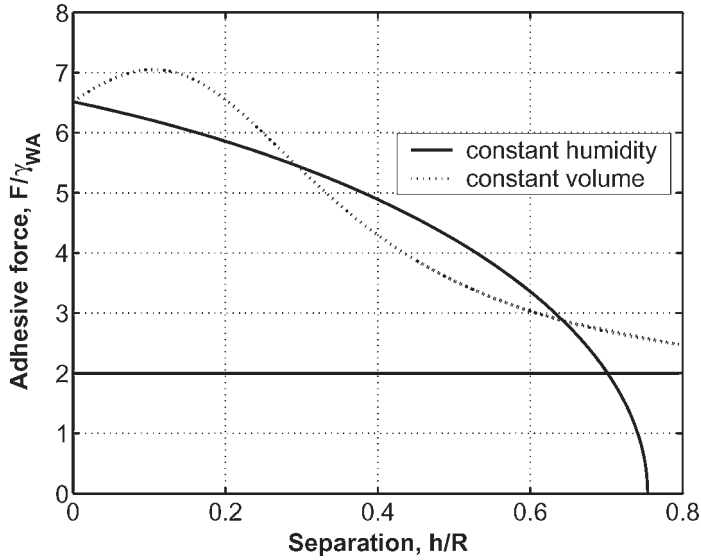

FIGURE 4 Adhesive force as it varies with separation for constant volume of water or constant curvature of the water/air interface.

Luckily, the adhesive force reaching $2\gamma_{WA}$ per unit length of the cylinder when the water bridge is broken in both cases is not a coincidence. From Equations (5) and (6) or (5) and (7), it is seen that the adhesive force is exactly equal to $2\gamma_{WA}$ when x_m is zero:

$$F_c = 2\gamma_{WA}. \tag{8}$$

This is independent of the contact angles, relative humidities, or the size of the cylinder. It is a surprising result that is very useful because we do not have to check x_m every time. We hope that something like this may be discovered for the sphere/plate contact.

The deformation is, of course, unstable if a force decreases while moving in the direction of application [26, 27]. In the pull-off test in this case, the force measured is the maximum force for the constant volume test and the initial force for the constant humidity test. So, it will be somewhat larger at constant volume than at constant humidity or the radius of curvature. However, the difference gets smaller when r/R gets smaller. In fact, the difference disappears at some critical r/R as shown in Figure 5. For all practical purposes, the pull-off force will be the same for both constant volume and constant humidity when r/R is less than 0.01. Because the RH depends only on r, this ratio depends on both the RH and the radius of cylinder.

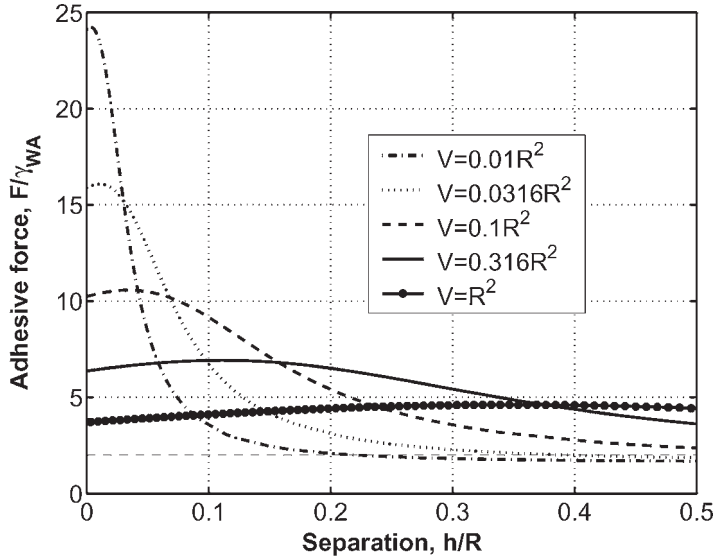

FIGURE 5 Effect of initial water volume or humidity on the adhesive force separation relationship at constant volume of water. The volumes of water from top to bottom at zero separation are shown corresponding to $r/R = 0.0285$, 0.0645, 0.153, 0.395, and 1.17, respectively.

Effect of Contact Angles

Figure 6 shows the effect of contact angles. When the contact angles increase from 0, the adhesive force decreases but remains at $2\gamma_{WA}$ when the bridge is broken independent of the contact angles. For both contact angles at $\pi/2$, the radius of curvature is negative or concave for water. This radius is small in the beginning ($-0.5\,R$) and increases in magnitude with separation. Its contribution to the adhesive force is negative or it tends to separate the cylinder from the plate. This contribution diminishes with separation and at about $h = 0.2\,R$ it balances the surface tension force so the total is zero. However, the water bridge is not broken. Upon continued separation, the surface-tension force becomes the major force that attracts the cylinder toward the plate. When this force reaches $2\gamma_{WA}$ the water bridge is broken, so the adhesive force drops suddenly to zero. Of course, when r is negative, the water vapor must be supersaturated. It could mean that water is introduced into the gap and evaporation is prohibited. For this case, the separation is a stable process. The separation starts with a negative force, goes through zero, and changes to a positive force

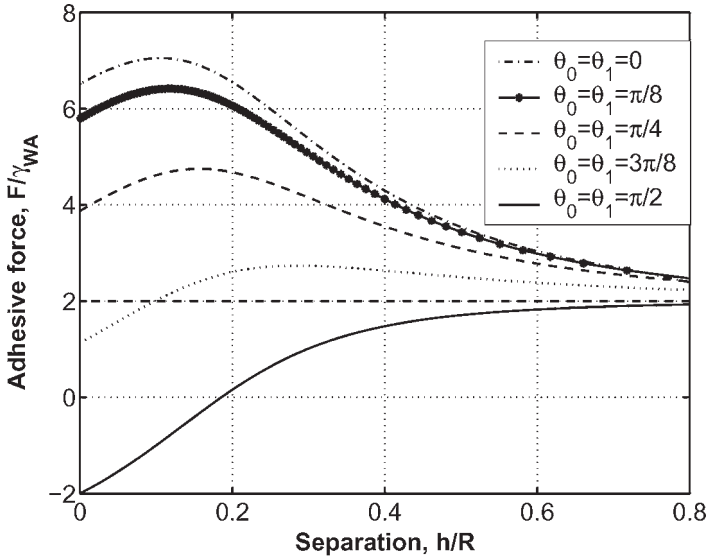

FIGURE 6 Effect of contact angles on the adhesive force separation relationship. The initial water volume is $0.3R^2$, which is maintained constant during separation.

approaching $2\gamma_{WA}$. At constant volume of water, the water bridge will never be broken in this case.

For hydrophobic surfaces in which the contact angles are larger than $\pi/2$, the situation is shown in Figure 7. The adhesive force starts as negative when the radius of curvature is negative or the water surface is convex. Then, it goes through zero and changes to positive when the surface tension force becomes dominant. Here, however, the water bridge disappears when ψ becomes zero as shown in Figure 8. At this time the adhesive force becomes zero suddenly, although there is no sign of such events in Figure 7. The pull-off force in all the situations is shown in Table 2. The pull-off force is all positive except for $\theta_0 = \theta_1 = \pi$, in which case it is zero. For the first four cases, the pull-off force is the maximum adhesive force after which the deformation is unstable. For $\theta_0 = \theta_1 = \pi/2$, the deformation is stable all the way with the water bridge intact until separation, at which time the adhesive force is $2\gamma_{WA}$ per unit length of the cylinder. For the last four cases, the water bridge is broken at the h/R shown where the angle ψ becomes zero. The adhesive force is positive even though the surfaces are hydrophobic unless $\theta_0 = \theta_1 = \pi$. On the other hand, the radii of curvature of the water/air interface for the latter cases are all negative,

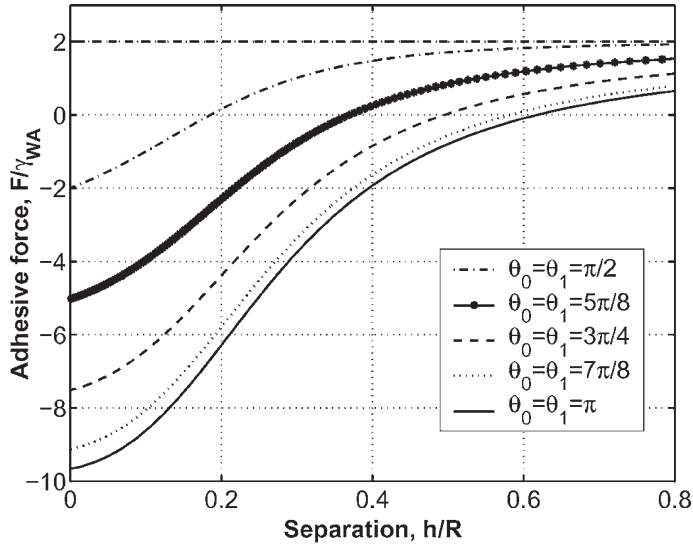

FIGURE 7 Effect of contact angles on the adhesive force–separation relationship. The initial water volume is $0.3R^2$, which is maintained constant during separation.

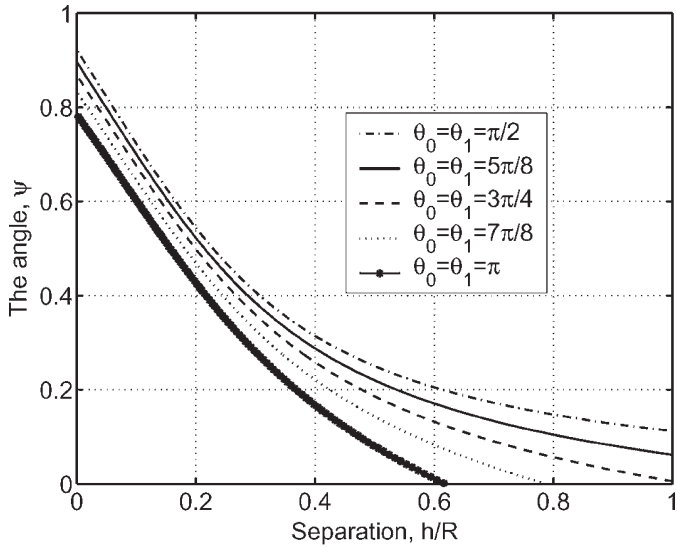

FIGURE 8 Effect of contact angles on the angle ψ–separation relationship. The initial water volume is $0.3\ R^2$, which is maintained constant during separation.

TABLE 2 The Pull-Off Force as a Function of Contact Angles for a Constant Water Volume of $0.3R^2$

$\theta_0 = \theta_1$ rad	$\theta_0 = \theta_1$ deg	h/R	r/R at $h = 0$	F/γ_{WA}
0	0	0.11	0.32	7.05
$\pi/8$	22.5	0.12	0.37	6.41
$\pi/4$	45	0.16	0.66	4.75
$3\pi/8$	67.5	0.29	−6.91	2.74
$\pi/2$	90	∞	−0.50	2.00
$5\pi/8$	112.5	1.50	−0.27	1.85
$3\pi/4$	135	1.03	−0.27	1.41
$7\pi/8$	157.5	0.79	−0.17	0.77
π	180	0.52	−0.16	0.00

indicating the equilibrium water vapor must be supersaturated or there is no equilibrium between water and its vapor. In other words, for the hydrophobic surfaces, no water will condense at the contact point under normal (0 to 100%) relative humidities. The adhesion would be between the solid surfaces without water.

Adhesion between Two Identical Cylinders

If $\theta_0 = \pi/2$, the situation is the same as two identical cylinders separated by $2h$ with twice the water volume. The adhesive force–separation relationship is shown in Figure 9. It is similar to the case of cylinder/plate adhesion. However, the radius of curvature may change sign during the separation process. For example, when $\theta_1 = 3\pi/8$, the radius of curvature starts at $-0.1\,R$ (see Figure 10), decreases all the way to $-\infty$ at slightly less than $h/R = 0.367$ and then changes to $+\infty$ at slightly more than $h/R = 0.367$, and decreases to a minimum of $5.125\,R$ at $h/R = 0.725$ and then increases slightly. The critical separation at which the radius of curvature changes sign is given by

$$\frac{h}{R} = \frac{(V/R^2) + (\pi/2) - \theta_1}{2\cos\theta_1} - 1 + \frac{1}{2}\sin\theta_1. \tag{9}$$

Here V/R^2 is 0.3. So, for $\theta_1 = \pi/4$, $h/R = 0.121$, and for $\theta_1 = 3\pi/8$, $h/R = 0.367$. Yet, such change of sign is not apparent from the curves in Figure 9.

For constant humidity or the radius of curvature, the effect of contact angles on the force–separation relationship between two identical cylinders is shown in Figure 11. It is seen that all such separation

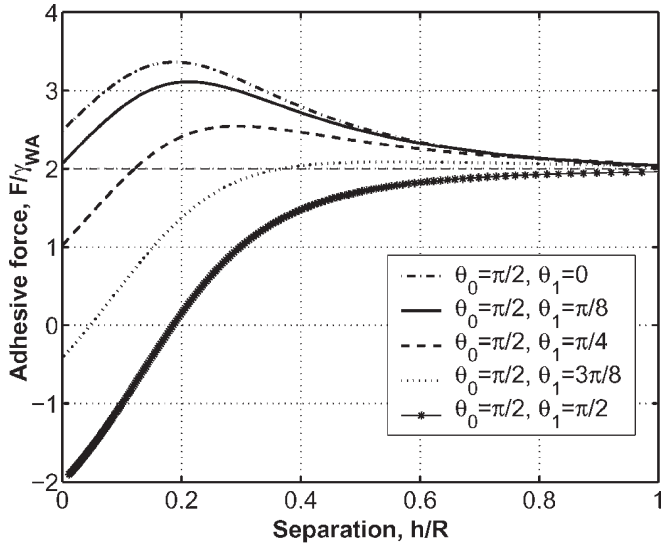

FIGURE 9 Adhesive force–separation relationship for $\theta_0 = \pi/2$ and from top to bottom $\theta_1 = 0$, $\pi/8$, $\pi/4$, $3\pi/8$, $\pi/2$ with the water volume maintained constant at $0.3R^2$. This is the same situation as that of two identical cylinders separated by $2h$ with a water volume of $0.6R^2$.

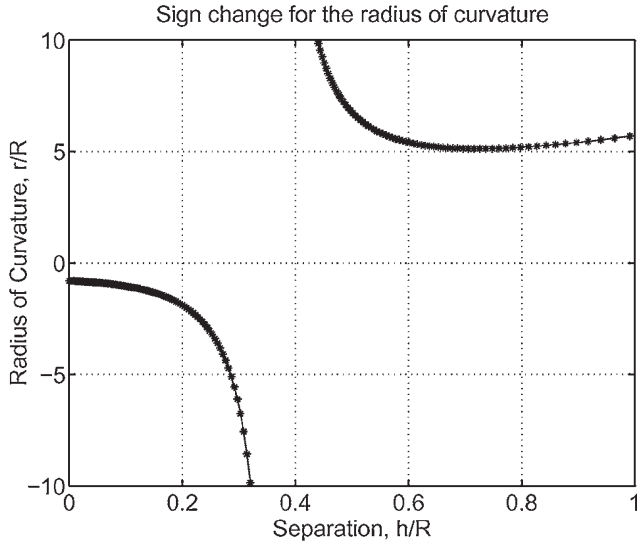

FIGURE 10 Sign change in the radius of curvature during separation for the case of $\theta_0 = \pi/2$ and $\theta_1 = 3\pi/8$. (The fourth line from top in Figure 9).

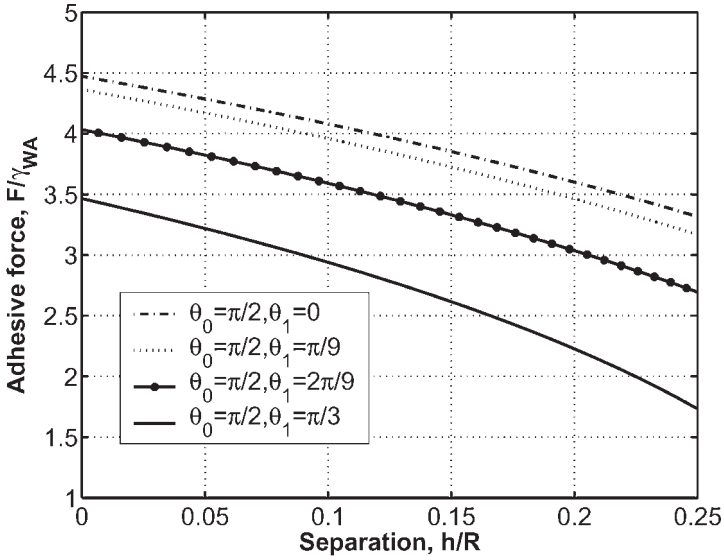

FIGURE 11 Adhesive force–separation relationship for $\theta_0 = \pi/2$ and various θ_1 values with the radius of curvature maintained constant at $r/R = 0.5$. This is the same situation as that of two identical cylinders separated by $2h$ with a water volume of $2V$ in the bridge.

processes are unstable because the force decreases with separation. So, the pull-off force is independent of the contact angles at $h = 0$. For $\theta_1 = \pi/3$, the water bridge is broken when $x_m = 0$ at $h/R = 0.225$ as shown in Figure 12. At this time the adhesive force is equal to $2\gamma_{WA}$ and then suddenly becomes zero. This happens before the volume of water becomes zero at $h/R = 0.232$ or $\psi = 0$ at $h/R = 0.250$, both of which can break the water bridge.

EFFECT OF RELATIVE HUMIDITY ON THE PULL-OFF FORCE

In the case of constant RH, the pull-off force measured is $h = 0$ as shown in Figure 4. The separation process is unstable because the force decreases with separation. The variation of this pull-off force as a function of humidity is shown in Figure 13. What is plotted is the force (F/γ_{WA}) *versus* the radius of curvature (r/R). Because only r is related to the RH through Equation (1), the relation between r/R and RH depends on R. However, increasing r means increasing humidity for the same R. Hence, the adhesive force per unit length of the cylinder decreases with increasing humidity. For the same

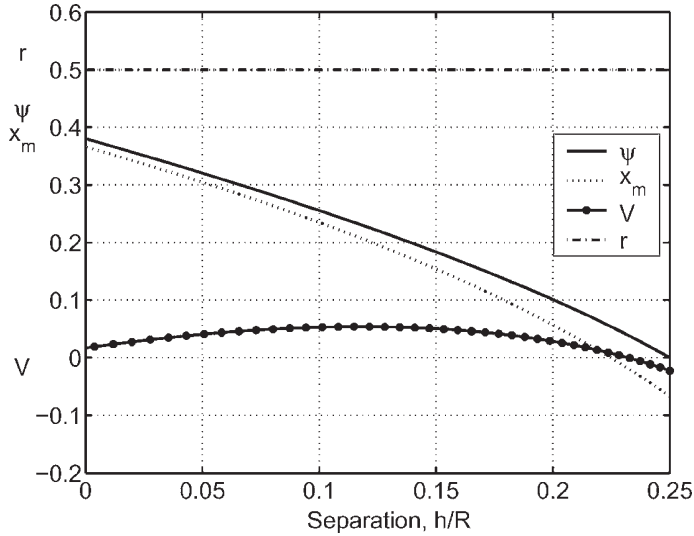

FIGURE 12 Angle ψ, the radius of curvature (r/R maintained at 0.5), the volume V/R^2, and x_m ($=x_0$ here) for $\theta_0 = \pi/2$ and $\theta_1 = \pi/3$. This is the same situation as that of two identical cylinders separated by $2h$ with a water volume of $2V$ in the bridge.

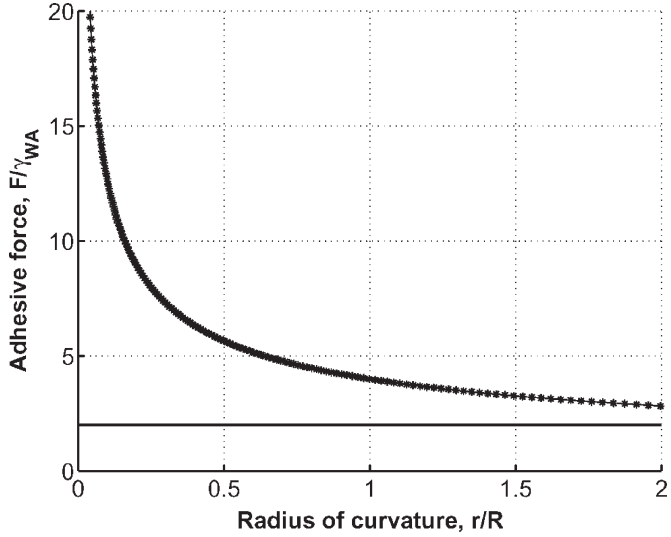

FIGURE 13 Adhesive or pull-off force as a function of the radius of curvature or relative humidity for $\theta_0 = \theta_1 = 0$.

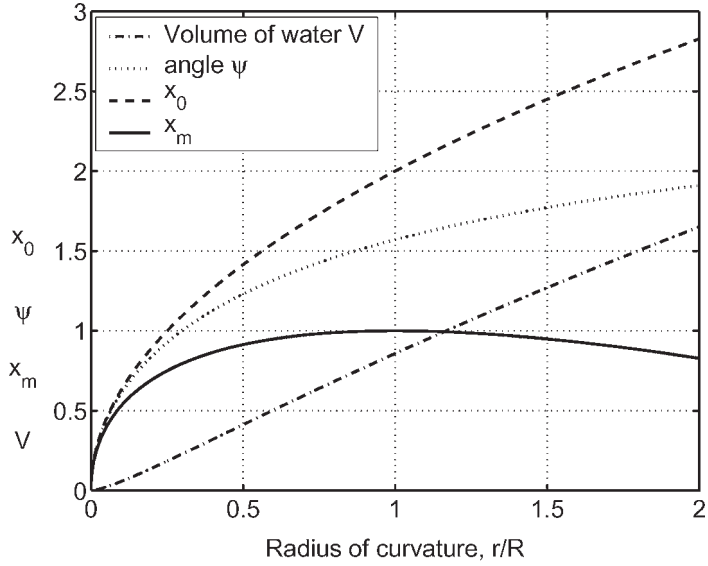

FIGURE 14 Volume of water, angle ψ, x_0, and x_m as a function of the radius of curvature of the water/air interface for $\theta_0 = \theta_1 = 0$.

curvature range the volume of water increases, the angle ψ increases, and x_0 increases with the radius of curvature as shown in Figure 14. For x_m it increases to a maximum of $1R$ at $r = R$ and then decreases. If the pull-off force is measured at constant volume of water, it would be somewhat larger as shown in Figure 5, but this difference disappears for small r.

When r is less than $0.1R$, the adhesive force at $h = 0$ is shown in Figure 15, and it approaches a straight line on a log-log plot for r less than $0.01R$. For very small r, the relations are simpler for $\theta_0 = \theta_1 = 0$:

$$\cos\psi = 1 - 2\frac{r}{R} \qquad \sin\psi = 2\sqrt{\frac{r}{R}} = \frac{x_0}{R} = \frac{x_m}{R} \tag{10}$$

$$\frac{F}{\gamma_{WA}} = 4\sqrt{\frac{R}{r}} \qquad \frac{V}{R^2} = \frac{8}{3}\left(\frac{r}{R}\right)^{3/2}. \tag{11}$$

These are shown in Figure 16. Because r is in nanometers for any usual humidity, cylinders measured in microns and up would be in this range.

The effect of contact angles other than zero is shown in Figures 17–20. In general the nonzero contact angles will reduce the pull-off

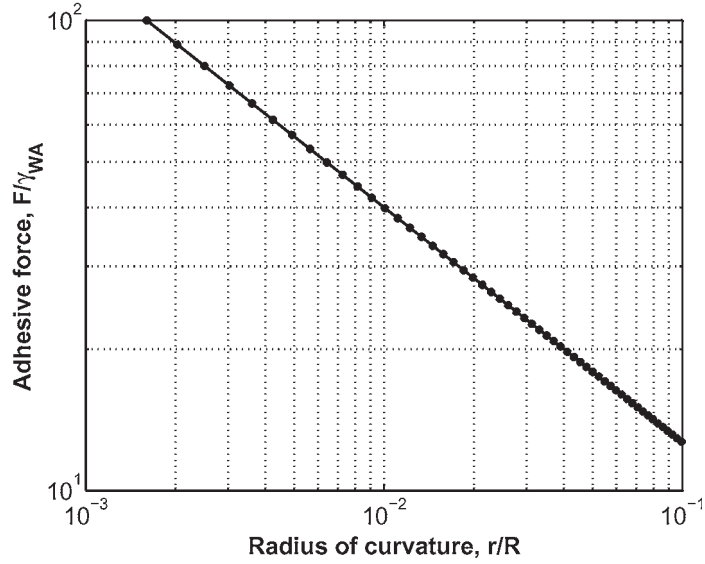

FIGURE 15 Adhesive force at low curvatures or low humidity for $\theta_0 = \theta_1 = 0$.

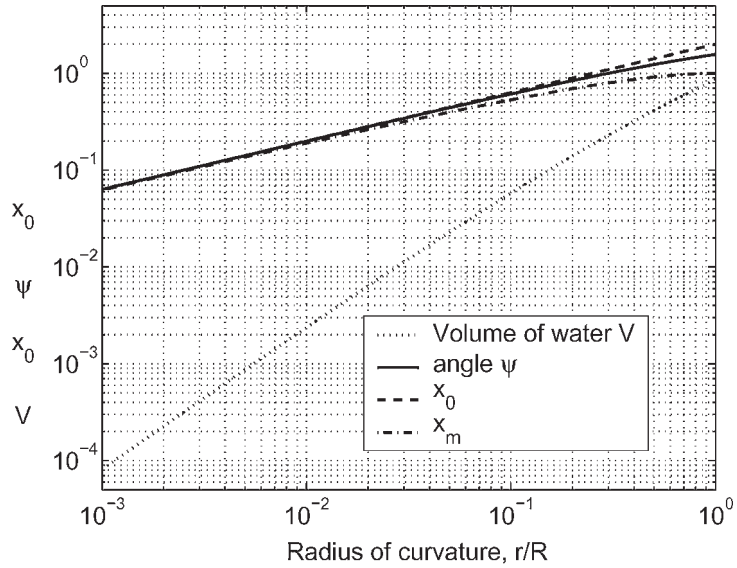

FIGURE 16 Volume of water V, angle ψ, x_0, and x_m at low curvatures for $\theta_0 = \theta_1 = 0$.

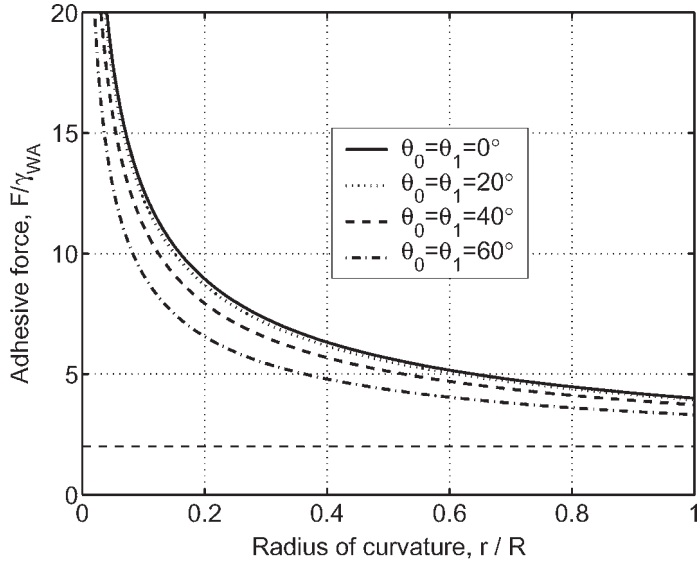

FIGURE 17 Adhesive force–curvature relationship for different contact angles. From top, $\theta_0 = \theta_1 = 0$, 20, 40, and 60 deg.

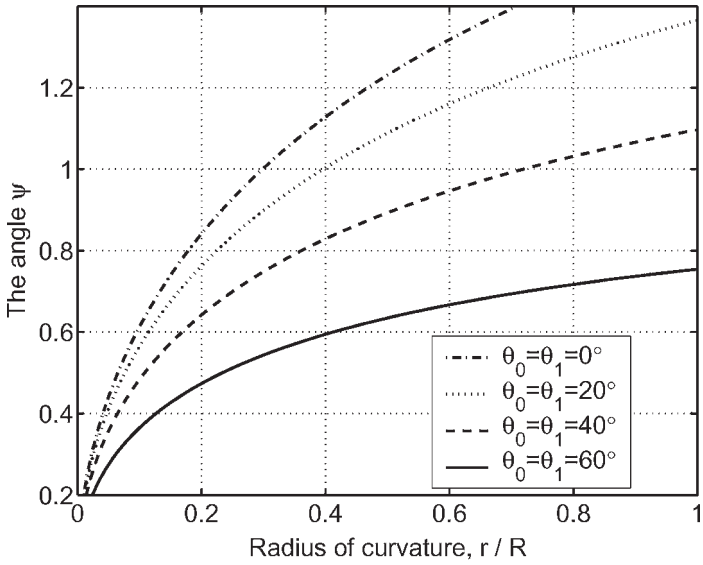

FIGURE 18 The relation between ψ and curvature for different contact angles. From top, $\theta_0 = \theta_1 = 0$, 20, 40, and 60 deg.

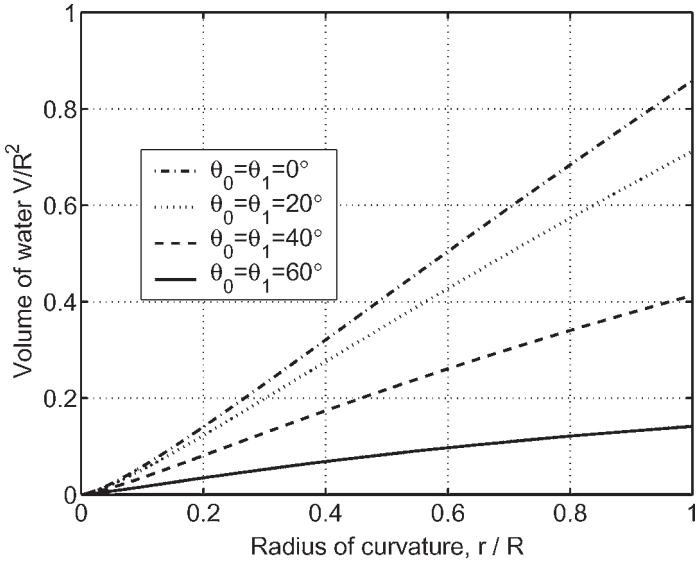

FIGURE 19 Volume of water–curvature relationship for different contact angles.

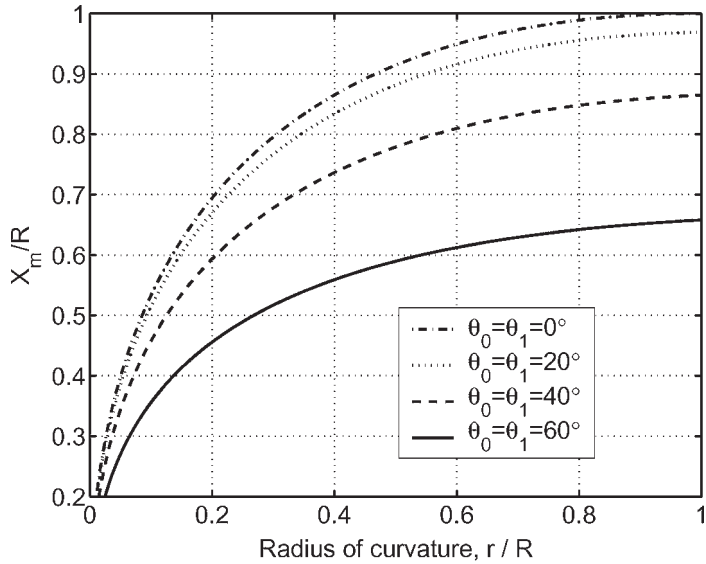

FIGURE 20 Closest x coordinate for the water bridge as it varies with the curvature for different contact angles. From top, $\theta_0 = \theta_1 = 0$, 20, 40, and 60 deg.

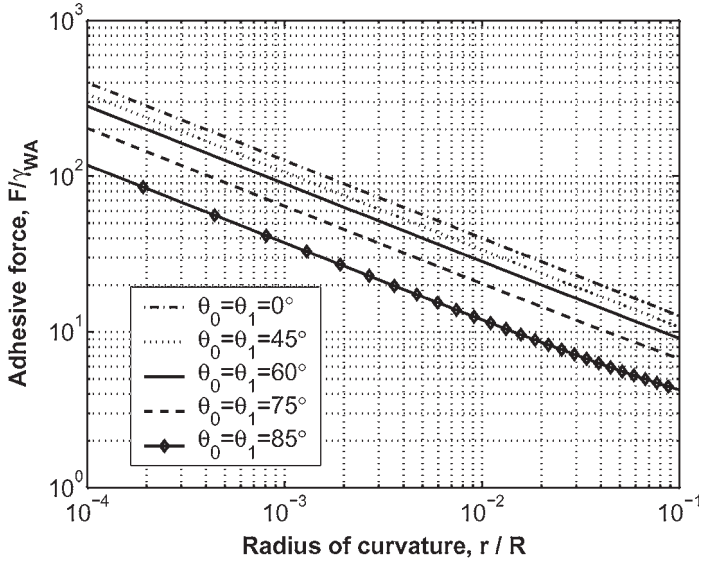

FIGURE 21 Adhesive force–curvature relationship at different contact angles for small radius of curvature or low humidity.

force as shown in Figure 17 for both contact angles of 0, 20, 40, and 60 deg. They also reduce the angle ψ for the same radius of curvature as shown in Figure 18. Because of that they also reduce the volume of water in the bridge as shown in Figure 19. For the same reason they also reduce the closest x_m coordinate but not enough to break the bridge as shown in Figure 20.

The relation between the pull-off force and the radius of curvature as shown in Equation (11) is plotted in Figure 21 for even lower relative humidities. The inverse square-root relationship holds not only for $\theta_0 = \theta_1 = 0$ but also for other angles. Note that the force increases continuously with decreasing humidity. However, it decreases with increasing contact angles. Similarly, the relation between the volume of water and the radius of curvature as shown in Equation (11) is plotted in Figure 22 to extend to even lower relative humidities. The exponent 1.5 works not only for $\theta_0 = \theta_1 = 0$ but also for other angles. However, the volume of water decreases with increasing contact angles.

For two cylinders or for a cylinder and a plate with $\theta_0 = \pi/2$, the pull-off force also increases with decreasing radius of curvature or RH as shown in Figure 23. However, it decreases with increasing θ_1, the contact angle between water and the cylinder.

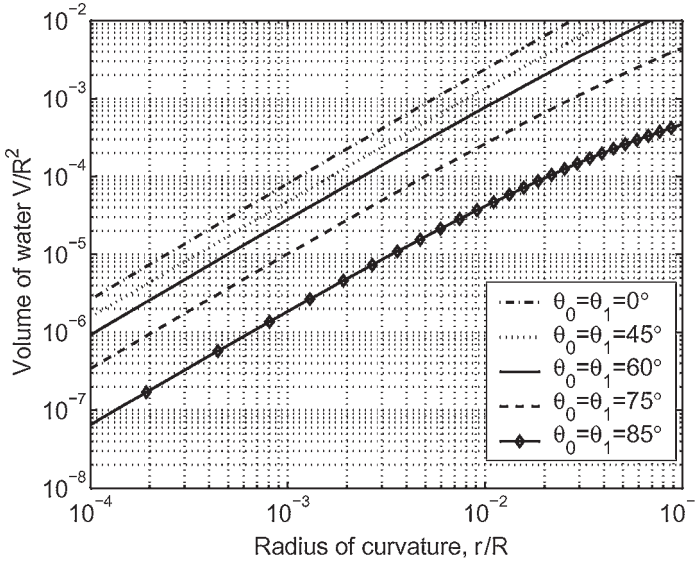

FIGURE 22 Volume of water–curvature relationship at different contact angles for small radius of curvature or low humidity.

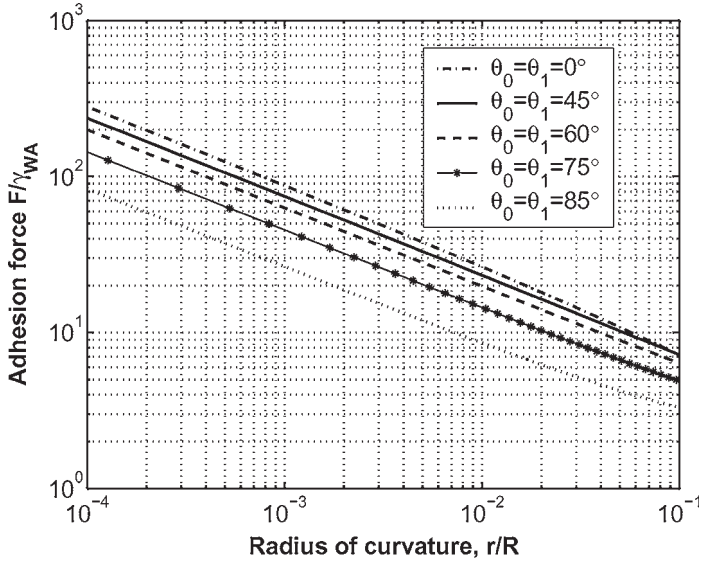

FIGURE 23 Adhesive force–curvature relationship between two cylinders at different contact angles for small radius of curvature or low humidity. Also for cylinder and plate for $\theta_0 = \pi/2$.

EXPERIMENTAL VERIFICATION

Because we had some difficulty in maintaining equilibrium for a water bridge, we performed a series of experiments using silicone oil instead of distilled water. The silicone oil from Dow Corning (Midland, MI, USA) had a specific gravity of 0.970 and a surface tension of 21.2 mN/m m at 25°C in air. The cylinder was a Corning Pyrex® glass tube, VWR, West Chester, PA, USA, 7 mm in diameter and 10 cm in length. The two ends of the tube were connected to a compumotor drive (SX6 from Parker Hannifin Corp., Rohnert, Park, CA, USA.) through a single silk thread passing through the center of the tube. The compumotor was mounted on an aluminum frame. The motor can be controlled to move the glass tube up and down at a constant velocity.

It is critical to keep the glass tube parallel to the glass plate during detachment. It is also critical that the oil bridge between the glass tube and glass plate is uniform along the length. To approach these goals, the glass tube was placed on a glass plate already covered with a uniform, thin layer of silicone oil. To make sure that the oil covered the glass plate uniformly, the coated plate was allowed to sit horizontally long enough so that the oil surface was as shiny as a mirror. Then, the glass tube was carefully detached from the oil-covered glass plate so that the glass tube acquired a thin uniform line of silicone oil along its length. Finally, the glass tube with the oil was placed carefully over a clean glass plate already sitting on the balance (Adventurer from Ohaus Corp., Pine Brook, NJ, USA). The amount of oil was calculated by knowing the weight of everything with and without the oil. To see whether the glass tube was parallel to the glass plate, the glass tube was lifted by the compumotor drive to attempt to detach it from the plate. The oil tended to shrink from both ends of the tube. If the shrinkage was equal at the two ends, the tube was considered parallel to the plate. This observation was made a few times to make sure it was repeatable.

The system was allowed to stay attached for about 30 min before the detaching measurement. Because it would take some time for the oil bridge to change configuration, the detachment and attachment velocity was set at about 40 nm/s. Data (force and displacement) were collected every 100 s through a RS232 port. During recording, the contact angle between silicone oil and glass tube was measured to be 36 deg and that between silicone oil and glass plate was 25 deg. It turned out that the attachment curves were better behaved than the detachment curves.

Figure 24 shows a comparison between theoretical calculations and measurement data for a volume of 0.450 mm^3/mm of silicone oil. It is

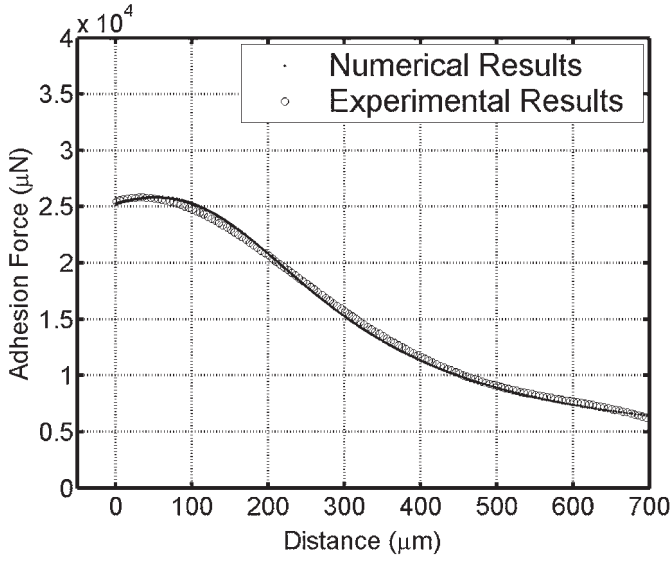

FIGURE 24 Adhesive force as it varies with separation for a constant volume of silicone oil.

clear that two curves agree with each other without any adjustable parameters. The adhesion force increases slightly to a maximum at 50-μm separation and then decreases continuously upon further separation. For an oil volume of $0.450\,\text{mm}^3/\text{mm}$ and $\text{R} = 3.5\,\text{mm}$, $V/R^2 = 0.037$. Figure 19 shows $r/R = 0.1$ for $\theta_0 = \theta_1 = 30\%$ and Figure 17 shows the adhesive force at $h = 0$ is $1.2\gamma_{WA}$ or $254\,\text{mN/m}$ (25.4 mN) for a 10-cm length. This can be compared with the observed value of 25.2 mN. Such agreement supports both our analysis and experimentation.

CONCLUSIONS

A cylinder and a parallel plate in contact may have water condensed between them in moist air. This is a source of adhesive force. Pulling them apart slowly is unstable if humidity is maintained constant during separation and if there is equilibrium between the water bridge and the humid air. Pulling them apart quickly can be stable initially and unstable afterward if the volume of water in the bridge is maintained constant so there is no equilibrium between the water bridge and the moist air. The region of stability diminishes with increasing curvature of the water bridge.

When the adhesive force is $2\gamma_{WA}$ per unit length of the cylinder, the water bridge is broken and the force suddenly becomes zero. This event does not show up in the calculated force–separation behavior.

Increasing contact angles reduces the adhesive force. For separation at constant volume of water, increasing the contact angles increases the stable region. The whole separation process can become stable. For $\theta_0 = \theta_1 = \pi/2$, the adhesive force is negative to start with and then becomes positive and separates at $2\gamma_{WA}$ per unit length of the cylinder.

When θ_0 is $\pi/2$, the situation is the same as two identical cylinders in parallel contact except that both the distance of separation and the volume of water must be doubled. For separation at constant volume of water, the curvature of the water/air interface can change sign during the separation process.

The adhesive force decreases with increasing RH, while the volume of water increases. For very small radius of curvature, the adhesive force per unit length of the cylinder increases as the square root of the radius of the cylinder for the same relative humidity. Increasing contact angles decreases the pull-off force.

In an experiment using a 7-mm glass tube in contact with a glass plate and using silicone oil instead of water to maintain constant volume, the force–separation relation agrees with the calculations without adjustable parameters, namely, using the measured contact angles and the surface tension reported in the literature.

ACKNOWLEDGMENT

This work was supported by the New York State Infotonics Center of Excellence. Skillful assistance from Chris Pratt and Joe Wodenscheck is gratefully acknowledged.

REFERENCES

[1] Bhushan, B. and Burton, Z., *Nanotechnology* **16**, 467–478 (2005).
[2] Tambe, N. S. and Bhushan, B., *Nanotechnology* **15**, 1561–1570 (2004).
[3] Tsukada, M., Irie, R., Yonemochi, Y., Noda, R., Kamiya, H., Watanabe, W., and Kauppinen, E. I., *Powder Technol.* **141**, 262–269 (2004).
[4] Liu, H. and Bhushan, B., *Ultramicroscopy* **100**, 391–412 (2004).
[5] Jones, R., Pollock, H. M., Geldart, D., and Verlinden, A., *Powder Technol.* **132**, 196–210 (2003).
[6] Yoon, E. S., Yang, S. H., Han, H. G., and Kong, H., *Wear* **254**, 974–980 (2003).
[7] Jones, R., Pollock, H. M., Cleaver, J. A. S., and Hodges, C. S., *Langmuir* **18**, 8045–8055 (2002).
[8] Rabinovich, Y. I., Adler, J. J., Esayanur, M. S., Ata, A., Singh, R. K., and Moudgil, B. M., *Adv. Colloid Interface Sci.* **96**, 213–230 (2002).

[9] He, M., Blum, A. S., Aston, D. E., Buenviaje, C., Overney, R. M., and Luginbuhl, R., *J. Chem. Phys.* **114**, 1355–1360 (2001).
[10] Xiao, X. and Qian, L., *Langmuir* **16**, 8153–8158 (2000).
[11] Sedin, D. L. and Rowlen, K. L., *Anal. Chem.* **72**, 2183–2189 (2000).
[12] Bhushan, B. and Dandavate, C., *J. Appl. Phys.* **87**, 1201–1210 (2000).
[13] Busnaina, A. A. and Elsawy, T., *J. Adhes.* **74**, 391–409 (2000).
[14] Xu, L. and Salmeron, M., *Langmuir* **14**, 2187–2190 (1998).
[15] Podczeck, F., Newton, J. M., and James, M. B., *J. Colloid Interface Sci.* **187**, 484–491 (1997).
[16] Eastman, T. and Zhu, D.-M., *Langmuir* **12**, 2859–2862 (1996).
[17] Hu, J., Xiao, X. D., Ogletree, D. F., and Salmeron, M., *Science* **268**, 267–269 (1995).
[18] Harnby, N., Hawkins, A. E., and Opalinski, I., *Tran. I. Chem. E.* **74**, 616–626 (1996).
[19] Thundat, T., Zheng, X. Y., Chen, G. Y., and Warmack, R. J., *Surf. Sci. Lett.*, **294**, L939–L943 (1993).
[20] Iida, K., Otsuka, A., Danjo, K., and Sunada, H., *Chem. Pharm. Bull.* **40**(1), 189–192 (1992).
[21] Opalinski, I., The effect of humidity of surrounding atmosphere on capillary adhesion forces in powders. "Modeling and critical humidity," *Inzynieria Chemiczna i Procesowa* **22**, 291–310 (2001).
[22] Marmur, A., *Langmuir* **9**, 1922–1926 (1993).
[23] de Lazzer, A., Dreyer, M., and Rath, H., *Langmuir* **15**, 4551–4559 (1999).
[24] Stifter, T., Marti, O., and Bhushan, B., *Phys. Rev.* **B62**, 13667–13673 (2000).
[25] Chaudhury, M. K., Weaver, T., Hui, C. Y., and Kramer, E. J., *J. Appl. Phys.* **80**(1), 30–37 (1996).
[26] Maddocks, J. H., *Arch. Rat. Mech. Anal.* **99**, 301 (1987).
[27] Li, J. C. M., *Mat. Sci. Eng.* **A285**, 207–212 (2000).